Equilibrium crystal shape of Bi-saturated Cu crystals at 1223K

Dominique Chatain[1], Paul Wynblatt[2], Gregory S. Rohrer[2]

[1] Centre de Recherche en Matière Condensée et Nanosciences[*] – CNRS,
campus de Luminy, case 913, 13288 Marseille cedex 9, France
[2]Departement of Materials Science and Engineering, Carnegie Mellon University,
Pittsburgh, PA 15213-3890, USA

Keywords
Bismuth, Copper, Surface Segregation, Equilibrium Crystal Shape, Surface Energy.

Abstract
The equilibrium crystal shape of Bi-saturated Cu at 1223 K has been studied, after quenching the material to room temperature, by a scanning electron microscopy investigation of the shapes of pores (or negative crystals) that are present on grain boundary fracture surfaces. Bi-saturation of Cu surfaces at 1223 K results in dramatic changes in the ECS compared to pure Cu. Whereas all possible surface orientations are stable in the case of pure Cu, only the {111}, {100}, {110}, and {320} orientations are stable in Bi-saturated Cu crystals. In addition, the weak maximum anisotropy of pure Cu of 2% is increased four-fold by Bi saturation of the surface.

1. INTRODUCTION

The shape of a metallic crystal in equilibrium with its vapor phase has been the subject of considerable study. The equilibrium crystal shape (ECS) is directly related to the anisotropy of surface energy, which tends to be rather small in the most studied fcc metals, amounting to about 5% or less between surfaces of minimum and maximum energy [1-5]. In particular, a recent study of the ECS of pure Cu has reported that the maximum surface energy anisotropy at 1240 K is only about 2% [5]. In contrast to pure metals, little effort has been devoted to the investigation on the ECS of the effects of adsorbed gas phase components, or of surface segregated solutes [6,7]. These limited studies have indicated large increases in anisotropy due to the presence of adsorbates, whether these are derived from the gas phase or by the equilibrium segregation of surface-active solutes from the bulk of the material. For a given adsorbate, the ECS is, of course, independent of the origin of the adsorption.

[*] Laboratoire Propre du CNRS associé aux Universités d'Aix-Marseille 2 et 3

In the present study, we have investigated the effects of Bi surface segregation on the Cu ECS at 1223 K. The Cu-Bi system has been widely studied because it displays grain boundary (GB) embrittlement [8,9] and grain boundary facetting [10,11] due to Bi GB segregation, as well as liquid metal embrittlement [12,13] as a result of wetting of Cu grain boundaries by Bi-containing liquid. A recent study of Cu polycrystalline surfaces has also revealed that Bi segregates strongly to Cu surfaces of all orientations [14]. This surface segregation is anisotropic, and varies from about 0.75 to 1 monolayer on the surfaces of different grains. In that study, it was observed that Bi segregation causes micro-faceting of almost all of the surfaces of polycrystalline Cu. The ECS of *pure* Cu displays small {111}, {100}, {110}, and possibly {113} facets, separated by rounded surfaces [5]. These rounded surfaces connect tangentially to the facets, so that all orientations are present on the Cu ECS. Pure Cu surfaces do not therefore display any unstable surface orientations susceptible to faceting. Thus, the observation that the surfaces of polycrystalline Cu are faceted in the presence of adsorbed Bi clearly indicates that Bi changes the anisotropy of the surface energy of Cu in a manner that renders most surface orientations unstable to faceting. In this paper, we report the effects of Bi adsorption on the ECS of Cu, from a study of the shapes of small pores in the Bi-saturated Cu.

2. EXPERIMENTS

A 99.995 % pure copper sample[•] in the form of a 14x9x2mm platelet, subjected to 95% cold work, was polished with 1μm Al_2O_3 and 0.02μm SiO_2. The sample was annealed for 18h at 1223K in an atmosphere of flowing hydrogen, in the presence of a Bi drop saturated with copper (located in the annealing furnace on another nearby copper platelet). Previous studies have indicated that heat treating similar Cu samples in hydrogen under the same conditions removes all sulfur and oxygen contamination from the sample [14]. During annealing in the presence of Bi, the pure copper sample undergoes Bi-saturation by vapor phase transport, without direct contact with the liquid. The solubility of Bi in solid copper has a maximum value (associated with retrograde solubility) of about 10^{-4} at 1223K [15]. Following equilibration in Bi vapor, the sample was quenched, and fractured. The resulting fracture occurred along the grain boundaries, and revealed the presence of small pores, which straddle the grain boundary and are split by the intergranular fracture path. These pores were found to be highly faceted, and

[•] containing 7ppm (by weight) O, 6ppm S, <0.5ppm Ag, <2ppm P, 6ppm Te, 5ppm Fe, 3ppm Sb, 4ppm Sn, 4ppm Ni, and 13ppm of additional elements with less than threshold levels.

represent "negative" crystals of Bi-saturated Cu. The shapes of pores present on the grain boundaries were investigated in a scanning electron microscope equipped with a field emission electron gun (FEG-SEM).

3. RESULTS AND DISCUSSION

3.1 Pore morphology

Although the origin of GB pores in Cu-Bi alloys is unknown, the presence of these pores allows the study of the equilibrium shape of the Bi-saturated Cu surfaces through the study of the partial negative crystals making up the pore.

Figures 1a and 1b show images of the two halves of a given pore, obtained from the two sides of an intergranular fracture. Each half-pore is strongly faceted by its equilibration in the presence of Bi vapor. The bright arc that crosses the pore in Fig. 1b is a slip band produced during sample fracture. Figures 1a and 1b also display bright contrasts, marked by white arrows, corresponding to a Bi-rich skirt unevenly split between the two sides of the intergranular fracture. The corresponding depressions left on opposite sides of the GB by the removal of the Bi-rich skirt are marked black arrows. All pores are rimmed with a Bi-rich skirt, indicating that the pores were in contact with Bi-containing liquid, and therefore filled with saturated Bi vapor at the chemical potential of Bi-saturated Cu corresponding to the equilibration temperature.

Figure 2a is a schematic of a GB pore. It shows the pore formed by two partial negative crystals, with a rim of Bi-containing liquid lying at the intersection of the two halves of the pore and the GB.

Since the two half-ECS's are misoriented with respect to each other, there will in general be a mismatch between the two shapes where they meet along the GB. The line of intersection of the two half-ECS's could therefore be quite complex. This is shown schematically in Fig. 2b, in which the black line represents the locus of the intersection of two half-cubo-octahedral pores twisted along a <100> axis by 30°. Recent calculations of the shapes of faceted particles lying on an *isotropic* GB have shown that a generally planar GB can pucker in the vicinity of its line of intersection with the particle, in a manner which depends on several factors, including the degree of wetting of the GB by the particle phase, as well as energy minimization of the respective interfacial energies [16]. However, the GB's in Cu-Bi are quite anisotropic, as indicated by the significant faceting of the GB's (see Figs. 1a and 3a). This faceting implies the existence of GB torques, which would tend to inhibit puckering of the GB to conform to the line of intersection of the two ECS's. These features might explain why a rim of Bi-containing liquid is found around each pore. The presence of a (relatively low surface energy) liquid

could provide a means of optimizing the interfacial energetics of a region where several high-energy junctions between rigid faceted interfaces would otherwise prevail.

3.2 Major facets

SEM images of several pores are displayed in Fig. 3. The pore size is largest in Fig. 3a and decreases progressively to Fig. 3e. The figure shows that facets are beginning to form in the largest pore (Fig. 3a) and are completely formed in the smallest pore (Fig. 3e). This apparently more rapid rate of equilibration of the smaller pores is consistent with the size dependence of shape equilibration kinetics by surface diffusion, which display a relaxation time proportional to the fourth power of pore radius, as discussed by Nichols and Mullins [17]. Thus, pore size may be considered to be a proxy for the temporal evolution of the faceting process.

In view of the sequence of progressively faster faceting of the pores with decreasing size, and hence the progressive faceting of any given pore with increasing time, we propose the following sequence of events. Pores are initially present at grain boundaries, before the arrival of Bi by GB diffusion from the sample surface. Their initial shapes are essentially consistent with the pure Cu ECS, shown in Fig. 4a. Fig 4 is an SEM image of a pure Cu crystal equilibrated at 1240 K, together with a schematic identifying the facets. The pure Cu ECS is made of small facets smoothly connected to curved surfaces.

For the purpose of the following discussion, a schematic of the Bi-saturated Cu ECS, consistent with the shape of Fig. 3e, is shown in Fig. 3f. The shape is shown to be fully facetted (no round parts) and is seen to consist of {100}, {111}, {320} and {110} facets. The Bi-saturated Cu ECS is quite different from the ECS of pure Cu, shown in Fig.4. It is clear that the presence of Bi at the Cu surface converts the ECS of pure Cu from one made up principally of curved surfaces with small facets to one that is essentially fully facetted.

3.3 Facet evolution

Going back to Fig. 3a (which corresponds to a relatively early stage in the faceting process) one sees small round {111}, small square {100}, and approximately rectangular {110} facets bordered on two sides by {320} facets. We will distinguish in the following discussion between the major, essentially flat, facets, and the surrounding regions, which contain faceted micro-steps or pyramids of limited spatial extent. These surroundings will be referred to as micro-facetted regions. The micro-facetted regions are most easily discerned in Fig. 3a surrounding the {320}-{110}-{320} sequences.

The {111}, {100} are already present on the pure Cu ECS, at approximately the relative dimensions shown in Fig. 4a. But the {110} facets, which are quite small and elliptical on the pure Cu ECS [5], have grown larger than in pure Cu, and their shape has been modified by contact on two sides with rapidly growing {320} facets not originally present on the pure Cu ECS. By the time equilibration is essentially complete (Figs. 3d and 3e) the {110} facets have almost disappeared. Thus, the small {110} facets present on pure Cu first grow, as Bi is adsorbed, and then almost vanish on the final Bi-saturated ECS by growth of the adjacent {320} facets.

The kinetics of facet size change depend on several factors, as described in more detail in Section 3.5.

3.4 Micro-facetted regions

The regions between the major facets on the final ECS are initially surrounded by micro-facets. The number of micro-facets gradually decreases with decreasing pore size, but the micro-facet size remains almost constant. For example, there are 5 micro-facetted steps between {320} and (100} in Fig. 3c, but only 3 steps in Fig. 3d, and only 1 or 2 in Fig. 3e.

Prior to Bi adsorption, the pore surfaces consist mainly of rounded regions that display all possible orientations. With the exception of the portions of those surfaces which correspond to {100}, {111}, {110} and {320} orientations, the rounded surfaces become unstable to faceting as Bi adsorption proceeds. The nature of the micro-facets, which develop on the unstable surface orientations, can be summarized in a so-called n-diagram [19,20], shown for the case of Bi-saturated Cu surfaces in Fig. 5a. The diagram is a stereographic projection in which stable surface orientations (i.e. the facet orientations) are represented by points. The line segments between the points run through the orientations that are unstable to decomposition into the two orientations at the ends of the segment, and the triangles enclosed by lines identify orientations which are unstable to decomposition into micro-facetted pyramids bounded by the three orientations at the corners of the triangles. Examples of micro-facetted structures from regions that decompose into two and three micro-facets, are also shown in Fig. 5. All of the micro-facets observed are consistent with a final ECS that is fully facetted, and which consists exclusively of {100}, {111}, {110} and {320} facets.

3.5 Kinetics of facetting

Two main factors are believed to be responsible for the kinetics of crystal shape equilibration. For crystals with an initially arbitrary shape it is possible to use the formalism of Nichols and Mullins [17] to estimate the relaxation time needed to form

facets by transporting material to or from the regions where they develop. The principles should not be any different for the case of a pore, or "negative" crystal, as long as pore volume is approximately conserved during shape equilibration. This formalism provides an estimate of equilibration time when diffusional processes are rate controlling, and yields a relaxation time for shape equilibration that depends on pore radius to the fourth power for the case of surface diffusion. However, the existence of a possible mechanism for kinetic inhibition of the equilibration process has recently been put forward by Mullins and Rohrer [21] and Rohrer *et al*. [22]. That work has shown that crystals which lack step propagating defects (such as dislocations with a screw component intercepting the faceted surfaces) will not equilibrate in reasonable times due to the existence of nucleation barriers which cannot be overcome by thermal activation.

In the present study, the kinetics are rendered more complex by the superposition of Bi transport processes onto the local shape equilibration of pores. Bi must first be transported through the vapor phase from the source to the sample, it must adsorb on the sample surface, diffuse down grain boundaries to the pores, and finally adsorb on pore surfaces, before any Bi-induced morphological changes can take place at the pore.

In addition, the potentially important role of a Bi-containing liquid skirt around the pores, which acts to facilitate the mutual accommodation of the rigid interfaces of the facetted half-pores and the GB, was discussed in Section 3.1 above. The Bi-Cu phase diagram [12] shows that the liquid in equilibrium with Bi-saturated Cu at 1223 K contains 17 at% Bi. Since the pore shape cannot fully equilibrate before such a liquid skirt has been formed, more Bi than would be needed to produce an adsorbed Bi layer at the pore surface is required to diffuse down the GB, in order to allow formation of the liquid phase. Since data are unavailable to evaluate the kinetics of all the various steps in the shape equilibration process, it is not possible to make detailed estimates of the overall equilibration kinetics.

It should be noted, however, that data to assess the rate of equilibration of pure Cu crystallites by surface diffusion are available, and previous estimates for the case of pure Cu have shown [5] that an equilibration treatment of 18h at 1223K is sufficient to fully equilibrate crystallites of radii of 4 μm or smaller. Since the surface diffusivity of Cu is increased by four orders of magnitude by Bi-saturation at temperatures in the vicinity of 1223 K [23], the present equilibration treatment should have been more than sufficient for shape equilibration by surface diffusion.

The only concern in the context of shape equilibration in the present experiments arises from the possible inhibition of the kinetics of facet growth by nucleation barriers, which could prevent the smallest pores from reaching their true equilibrium shapes.

Based on the typical dislocation density of a well-annealed metal (~$10^{11}/m^2$), one expects that pores with radii of $r \geq 4$ μm would have facets intercepted by one or more dislocations, on average. Facet growth or shrinkage in such large pores should not experience nucleation inhibition, since dislocations with a screw component will provide permanent surface steps, which preclude the need for repeated formation of new step nuclei. Therefore, the facets in pores 4 μm or more in radius should be able to achieve equilibrium-sized facets without inhibition. Facets in pores smaller than 1 μm are unlikely to be threaded by dislocations, so that their facet size could be inhibited. In the intermediate size range, where some facets would be threaded by dislocations, and others would not, one would expect threaded facets to have reached their equilibrium size, while unthreaded facets to be stunted in their growth, i.e. some significant size differences should be apparent among facets with identical indices, with resulting pore-shape asymmetries. This is not seen in the photos displayed in Fig. 3. Thus, it appears that nucleation inhibition may not be playing its expected role in this material. This may be due to the strong reduction in step energy produced by Bi adsorption at step edges, and consequent decrease in the barrier associated with step nucleation.

3.6 Apparent Equilibrium Shape

Assuming that Fig 3e does indeed represent the ECS of Bi-saturated Cu, we have quantified the shape of the smallest pores by fitting their shapes using the Wulffman software [18]. This was performed by modifying the relative distance between each type of facet and the Wulff point, until reasonable agreement was obtained based on visual examination. The result is shown in Fig. 3f. The relative values obtained in this manner for Bi-saturated Cu are:

$$\gamma\{100\} / \gamma\{111\} = 1.07,\ \gamma\{320\} / \gamma\{111\} = 1.06,\ \gamma\{110\} / \gamma\{111\} = 1.08$$

For comparison, the relative surface energies in pure Cu are:

$$\gamma\{100\} / \gamma\{111\} = 1.0024,\ \gamma\{110\} / \gamma\{111\} = 1.016,\ \gamma max / \gamma\{111\} = 1.02$$

Thus, under the assumption that the shapes obtained for the smallest pores reasonably approximate the ECS, we find that Bi adsorption leads to significant changes in the anisotropy of Cu.

3.7 General Remarks

There are numerous statements in the literature regarding the expected effects of adsorption (or segregation) on surface energy anisotropy. The general consensus seems to be that adsorption should decrease the anisotropy. This expectation seems consistent with considerations of the Gibbs adsorption isotherm. If several orientations are present on an ECS, then the overall surface energy of the crystal would most likely be reduced if adsorption were stronger on the surfaces of higher energy. This is because, in that case, the energies of higher energy surface orientations would be reduced more significantly than those of lower surface energy orientations, thereby decreasing the total energy as well as the overall anisotropy. Whereas the above reasoning undoubtedly applies in some cases, the present study provides evidence that such reasoning is not universally correct. An increase in surface energy anisotropy as a result of solute segregation has also been previously shown in the case of Pb crystals doped with Ni and Bi [7], and in the case of Cu crystals under the influence of oxygen adsorption [6].

4. CONCLUSIONS

Bi-saturation of Cu surfaces at 1223 K results in dramatic changes in the ECS compared to pure Cu. Whereas all possible surface orientations are stable in the case of pure Cu, only the {111}, {100}, {110}, and {320} orientations are stable in Bi-saturated Cu crystals. In addition, the weak maximum anisotropy of pure Cu of 2% is increased four-fold by Bi saturation of the surface. Thus, it is possible for solute segregation to increase the anisotropy of surface energy.

An unusual phenomenon has been observed in connection with the configuration of highly facetted pores at grain boundaries under conditions where a liquid phase can coexist with the solid phase. The need to accommodate the connection of two half-pores enclosed by rigid singular facets, with a facetted grain boundary, prompts the formation of liquid phase around the contact line, which presumably acts to optimize the intersection of these rigid interfaces.

Acknowledgments. The authors wish to acknowledge support of this research by the MRSEC Program of the National Science Foundation under award number DMR-0079996. One of us (DC) also wishes to thank the Carnegie Mellon University MRSEC for hosting an extended visit during 2003. Figure 2b was provided to us through the courtesy of Ellen J. Siem (Post-doctoral Fellow, CRMCN-CNRS).

References

[1] Heyraud JC., Metois JJ. Acta Metall. 1980; 28 : 1789

[2] Heyraud JC., Metois JJ. J. Cryst. Growth 1980; 50 : 571

[3] Heyraud JC., Metois JJ. Surface Sci. 1983; 128 : 334

[4] Wang Z, Wynblatt P. Surface Sci. 1998; 398 : 259

[5] Ghetta V, Chatain D, Wynblatt P, Interface Sci. 2004;12: 7

[6] Hondros ED, McLean M. CNRS conference report "La structure et les propriétés des
surfaces des solides", 1969;187: 219.

[7] Cheng W-C, Wynblatt P. J. Cryst. Growth 1997; 173: 513.

[8] Hondros ED, McLean D, Philos. Mag., 1974; 29: 771.

[9] Chang LS, Rabkin E, Straumal BB, Hofmann S, Baretzky B, Gust W. Defect Diff. Forum, 1998; 156:135.

[10] Ference TG, Baluffi RW. Scripta Metall. 1988; 22: 1929.

[11] Straumal BB, Polyakov SA, Bischoff E, Gust W, Baretzky B. Acta Mater. 2005; 53: 247.

[12] Joseph B, Barbier F, Aucouturier M. Scripta Mater.1998; 39: 775.

[13] Nicholas MG, Embrittlment by liquid and solid metals, Kamdar MH editor, TMS-ASM, 1982, p27.

[14] Chatain D, Wynblatt P, Rohrer GS, Scripta Mater. 2004; 50: 565

[15] Chang LS, Straumal BB, Rabkin E, Gust W, Sommer F. J. Phase Equilibria, 1997; 18: 128.

[16] Siem EJ, Carter WC, Chatain D. Phil Mag, 2004; 84: 991

[17] Nichols FA, Mullins WW. Trans. AIME 1965; 233: 1840

[18] Rosen AR, McCormack RP, Carter WC. Computational Mater. Sci. 1998; 11: 16

[19] Handwerker CA, Vaudin MD, Blendell JE. J. Phys. 1988; 49 C5: 367.

[20] Cahn JW, Handwerker CA. Mater. Sci. Eng. 1993; A192: 83

[21] Mullins WW, Rohrer GS, J. Amer. Cer. Soc. 2000; 83: 214

[22] Rohrer GS, RohrerCL, Mullins WW. J. Amer. Cer. Soc., 2001; 84: 2009

[23] Delamare F, Rhead GE. Surface Sci, 1973; 35: 172.

Figure Captions

Figure 1. (a) and (b) Two halves of the same pore from opposite sides of a GB fracture surface. Note the misorientation of the faceted features of the two half-pores, and the complementary parts of the Bi-skirt which has been split unevenly by the fracture path. Black and white arrows point to complementary parts of the liquid skirt around the pore (see text).

Figure 2. (a) Sketch of a pore at a Bi-saturated Cu GB showing the liquid skirt at the connection of the GB with the two half-surfaces of the pore (b) Schematic of the intersection (dark line) of two cubo-octahedra after relative rotation by 30° about an axial <100> direction. Courtesy E.Siem

Figure 3. (a) to (e) Series of half-pore shapes of decreasing size. (f) Schematic of the ECS of Bi-saturated Cu, produced using the Wulffman software [18].

Figure 4. (a) Equilibrated pure Cu crystal at 1240 K, in which the connections between the flat facets and the curved surfaces are tangential. (b) Schematic of the ECS of pure Cu produced using the Wulffman software [18]; this displays the relative facet size.

Figure 5. (a) n-diagram corresponding to the micro-faceting observed in pores. Photomicrographs illustrating microfaceting in the vicinity of different facet orientations: (b) vicinity of {100}; (c) vicinity of {111}; (d) vicinity of {110} in a large pore; (e) vicinity of {110} in a small pore.

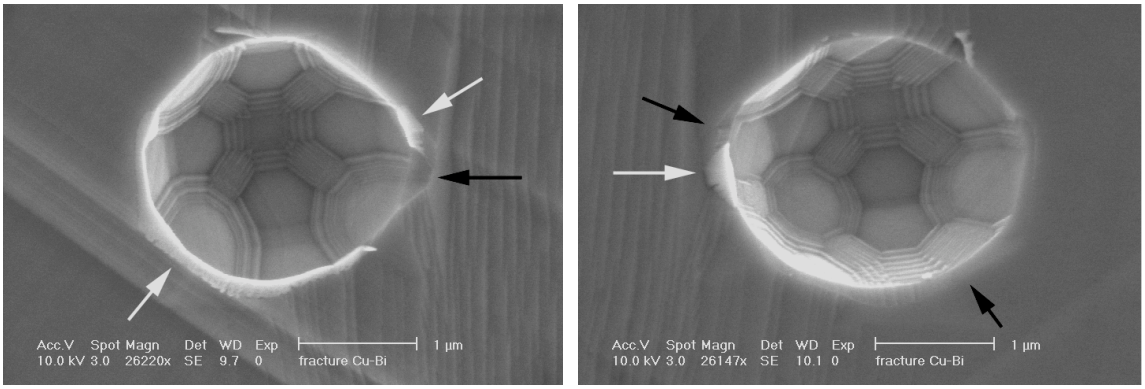
Acc.V Spot Magn Det WD Exp
10.0 kV 3.0 26220x SE 9.7 0
1 µm
fracture Cu-Bi
Acc.V Spot Magn Det WD Exp
10.0 kV 3.0 26147x SE 10.1 0
1 µm
fracture Cu-Bi

a b

Figure 1

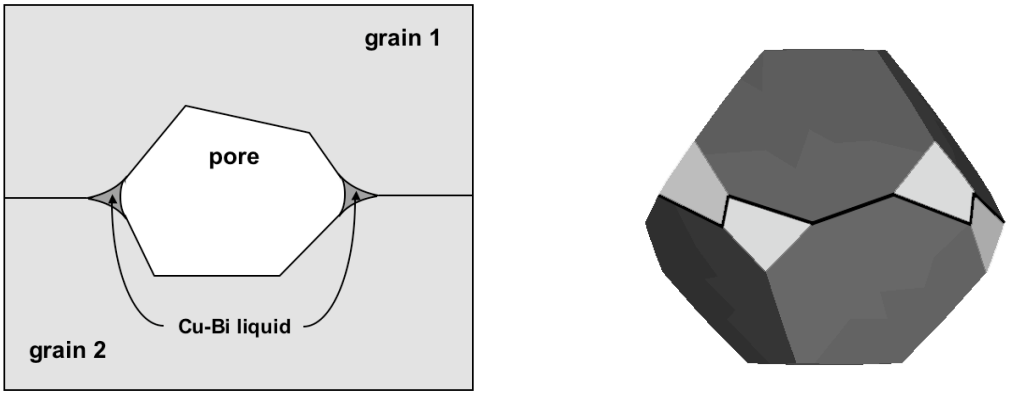

a b

Figure 2

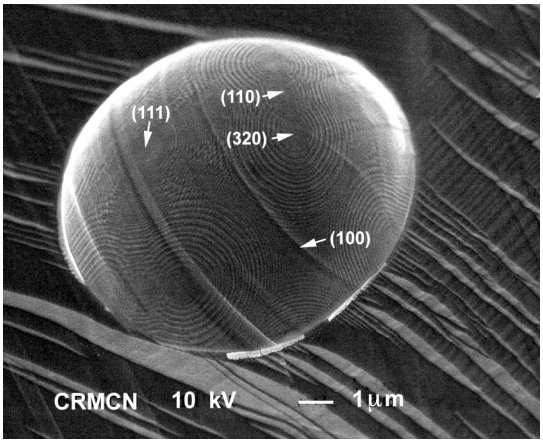

a

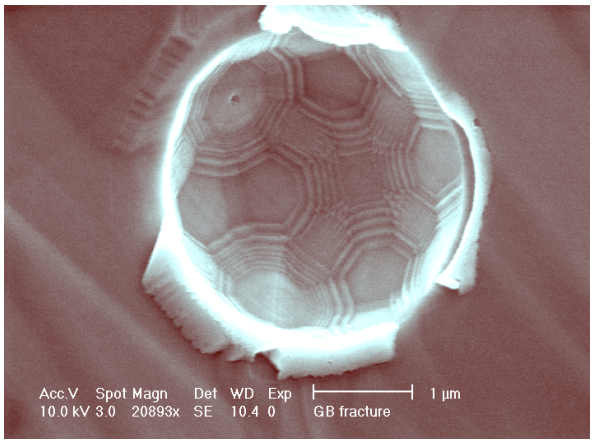

b

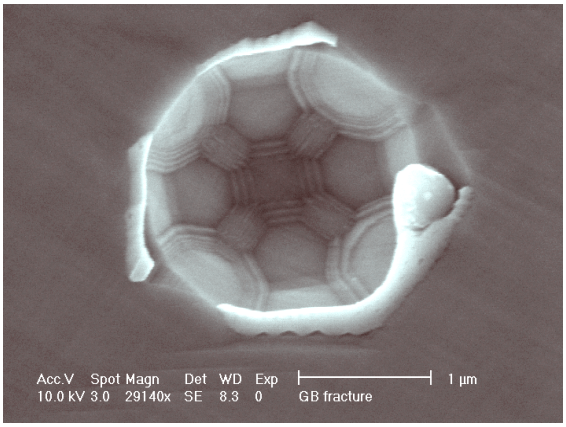

c

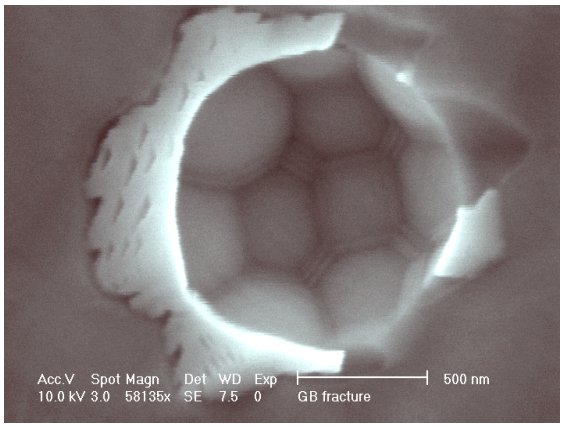

d

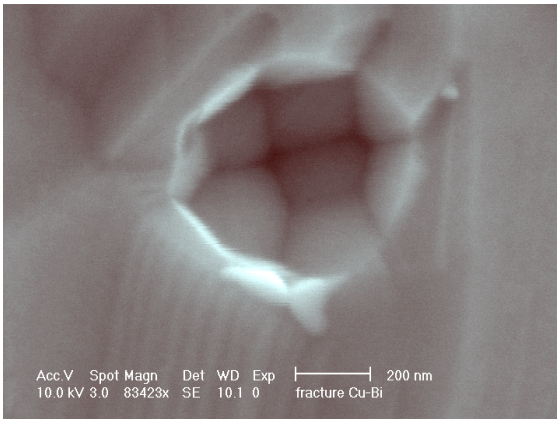

e

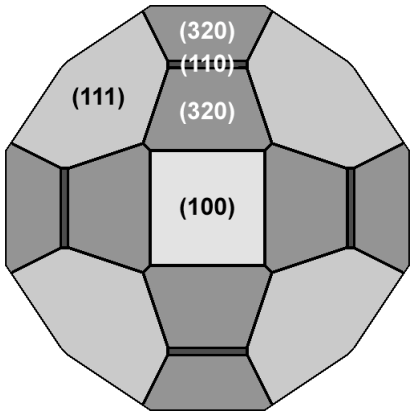

f

Figure 3

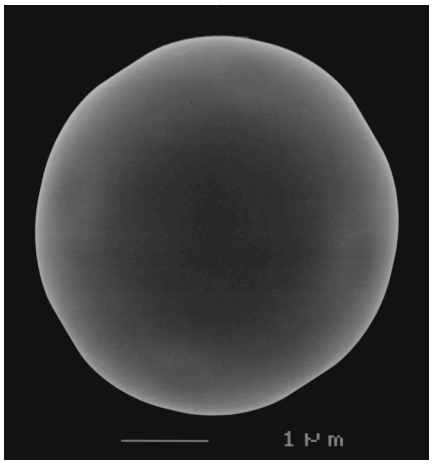

a

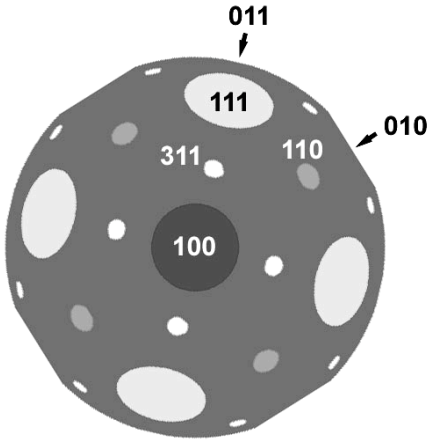

b

Figure 4

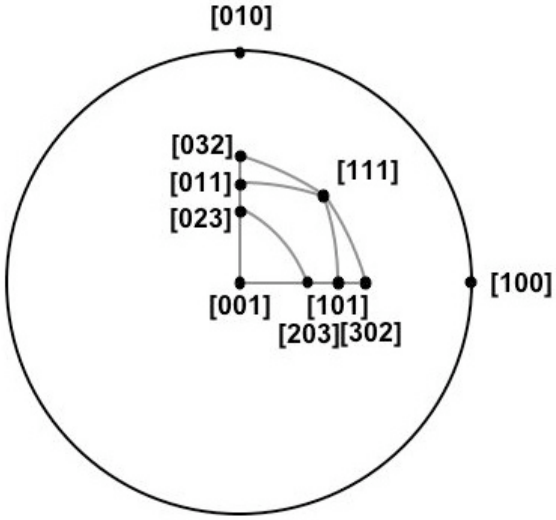

a

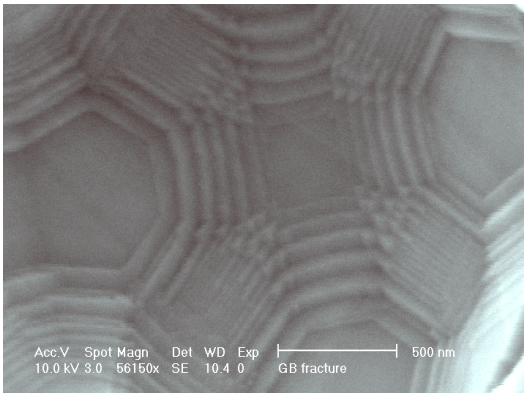

b

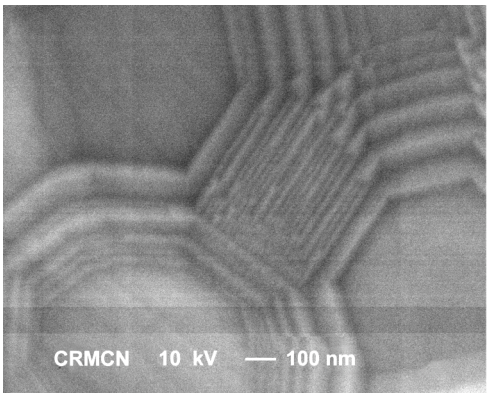

c

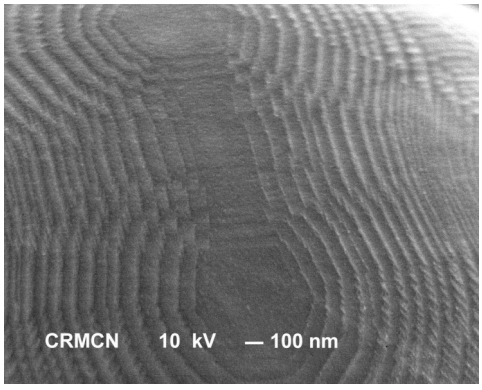

d

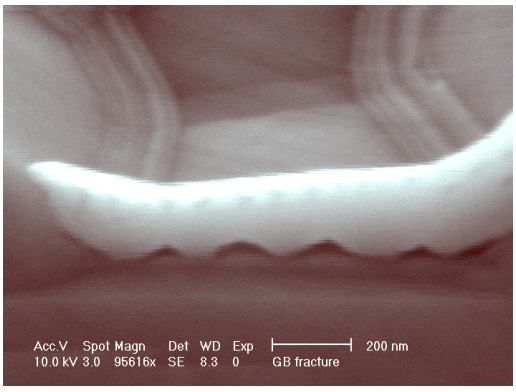

e

Figure 5